Journal of Molecular Liquids 348 (2022) 118023

Contents lists available at ScienceDirect

Journal of Molecular Liquids

journal homepage: www.elsevier.com/locate/molliq

Water sorption by ionic liquids: Evidence of a diffusion-controlled sorption process derived from the case study of [BMIm][OAc]

Alex Spieß, Philipp Brandt, Alexa Schmitz, Christoph Janiak *

Institut für Anorganische Chemie und Strukturchemie, Heinrich-Heine-Universität Düsseldorf, 40204 Düsseldorf, Germany

ARTICLE INFO

Article history:
Received 28 July 2021
Revised 25 October 2021
Accepted 2 November 2021
Available online 14 November 2021

Keywords:
Ionic liquids
Water vapor sorption
Diffusion control
Imidazolium ionic liquids

ABSTRACT

The hydrophilicity of ionic liquids (ILs) could be exploited as desiccants or in sorption-driven heat transformation, yet reports of water sorption isotherms of pure ionic liquids are still scarce. Here, water sorption studies for the six pure hydrophilic ionic liquids with 1-ethyl-3-methylimidazolium $[EMIm]^+$ or 1-butyl-3-methylimidazolium $[BMIm]^+$ cations and acetate $[OAc]^-$, formate $[HCOO]^-$ or lactate $[Lac]^-$ anions show a steady and high water uptake with a small hysteresis between absorption and desorption over the relative pressure range of p/p_0 = 0 – 0.9 for the first time. Repeated static volumetric sorption measurements with different amounts or different surface area of the example IL [BMIm][OAc] reveal a slow and strongly diffusion-driven sorption process stemming from the absorption of surface-adsorbed water into the bulk IL. Extrapolation of the water uptake to very small IL amounts with negligible kinetic hindrance gives an equilibrium water uptake capacity of over 2100 mg/g(IL) at p/p_0 = 0.9. Gravimetric control experiments at a relative humidity of 75.5 % confirm the time-dependence with the IL surface area at the gas–liquid-interface and the amount of the IL to reach the equilibrium uptake of 1040 mg/g at p/p_0 = 0.75.

© 2021 Elsevier B.V. All rights reserved.

1. Introduction

Ionic liquids (ILs) are a field of high interest since their various properties make them suitable solvents in catalysis, for cellulose, for battery electrolytes and water absorption [1]. ILs are a class of molten salts defined with a melting point below 100 °C [2]. The hydrophilicity and hygroscopic nature of ILs can be tuned through the choice of cation and anion [3–4]. In imidazolium-based ILs, the acidic proton in the C2–position (see Fig. S1 for the numbering of the atoms) can form hydrogen bonds to water and thereby contributes to the hydrophilicity [5]. The miscibility of an IL with water is mostly determined by the anion [6]. ILs with carboxylate anions are typically completely miscible with water, whereas those based on the hexafluorophosphate or bistriflimide anion are immiscible with water [7]. But even water-immiscible ILs can absorb water from air [8–9]. The absorbed water will then change the physical and chemical properties of the IL [10].

The high hydrophilicity of some ILs can be exploited, for example by using them as desiccants [11] or as an alternative sorption material to lithium halide solutions in sorption-driven heat pumps or for thermal energy storage (see Fig. S2, Supporting Information for further explanations) [12–13]. The largest drawbacks of the usually used lithium halide solutions are their high corrosivity and the limited solubility of lithium halide in water, while water-miscible ionic liquids can be used in fractions up to 100 wt–% [12,14]. An important factor when using ILs in sorption-driven heat pumps is the resulting heat of dilution during the absorption process which is the usable energy. It could be shown that the ionic liquid 1–ethyl–3–methylimidazolium acetate ([EMIm][OAc]) delivers 13.3 kJ of energy, when one mole of water is absorbed into one liter of the IL, while this value for a saturated lithium chloride solution is only 7.2 kJ [13]. Furthermore, the reduction of the water vapor pressure in the water-solution of ILs is comparable to that of LiCl-solutions, which results in favorable low circulation rates in absorption-cooling-pumps [12,15]. Schaber *et al.* already constructed an absorption heat transformer using water and the ionic liquid 1–ethyl–3–methylimidazolium methanesulfonate ($[EMIm][MeSO_3]$) which yielded promising results based on the coefficient of performance (COP, ratio of delivered heating power and used electrical power), the circulation ratio and heat flow, but entailed a high technical effort [16].

The biggest hurdle for the use of ILs in sorption-heat-pumps is to overcome their comparably low long-term thermal stability, especially for hydrophilic ILs [17]. Conventional determination of the temperature for thermal stability by thermogravimetric analy-

* Corresponding author at: Institut für Anorganische Chemie und Strukturchemie, Heinrich-Heine-Universität Düsseldorf, 40204 Düsseldorf, Germany.
E-mail address: janiak@uni-duesseldorf.de (C. Janiak).

https://doi.org/10.1016/j.molliq.2021.118023
0167-7322/© 2021 Elsevier B.V. All rights reserved.

sis (TGA) greatly depends on the used amount of the IL as well as of the heating rate, which can be explained by the slow heat transfer [18]. As a result, the decomposition temperature of ILs can be up to 100 °C lower than that determined by the onset-temperature during TGA with normal heating rates of 5 K min^{-1} [19]. Imidazolium acetate ILs already show a steady mass loss when heated constantly at temperatures as low as 100 °C. ILs with alkyl sulfate anions slowly decompose to bisulfate and the corresponding alcohol starting at temperatures of 120°°C [20–22].

Another potential application for hydrophilic ILs is the use as drying agents for gases. Acetate based ILs were shown to be better absorbents for water than silica gel or magnesium sulfate, but show a considerably lower water uptake when compared to phosphorous pentoxide (P_4O_{10}). However, ILs are easily regenerable by drying, other than P_4O_{10} [11]. A very important property, especially for drying purposes, is the maximum water sorption capacity of the ILs. The process of water sorption can be divided into three steps: (I) adsorption of water at the IL surface, (II) absorption of water into the IL by diffusion, (III) formation of water-ion complexes.

The adsorption of water at the IL surface (I) is mainly controlled by the alkyl chain length on the cation, since imidazolium salts tend to orient the alkyl chains away from the surface, resulting in stoichiometrically more alkyl chains found at the surface than expected [9]. Regarding the absorption of water into the bulk IL (II), there is no consensus whether this process is the rate-limiting step in water sorption [23] or not [12]. By using ambient pressure X-ray photoelectron spectroscopy (APXPS) it was suggested that the kinetics of water adsorption at the gas–liquid-interface are considerably faster than the absorption of water into the bulk IL [24]. After the diffusion into the IL follows the formation of water-ion-complexes (III). At low water fractions, symmetrically H-bonded complexes of the type $A^-\cdots$H-O-H$\cdots A^-$ form (A^- representing the anion of the IL). At higher water fractions, water-water-interactions come into play, forming water-clusters inside the ionic liquid [25–26]. Furthermore, the IL itself builds up aggregates, creating hydrophilic and hydrophobic domains which are comparable to micelles [24,27–28]. This aggregation increases with the alkyl chain length on the cation but can already be observed with ethyl chains [29]. This pronounced self-organization is also observable in neat ILs, reducing the number of effective charge carriers and subsequently the expected conductivity [30].

Determination of the water sorption capacity is usually carried out by using the gravimetric method [9,11,23]. In this case, a defined amount of the ionic liquid absorbent is placed in a chamber with constant temperature and constant relative humidity. Then, the increase in mass of the absorbent is detected by an analytical balance, with the increase being a result of water absorbed from the atmosphere. The disadvantage of this method is that the sorption capacity can only be determined for one static condition at a time and not for a continuous range of partial water vapor pressure, so the literature on complete water sorption isotherms of pure ionic liquids is still scarce [8,31–33]. Radakovitsch *et al.* recently reported water sorption isotherms using the volumetric method for the (supported) ionic liquid [EMIm][$MeSO_3$] coated on silica gel for gas dehydration, showing very high water loadings at high relative pressures [34–35].

In this work the volumetric vapor sorption method was used to measure water sorption isotherms of six selected hydrophilic ionic liquids for the first time, including complete absorption and desorption branches. The ionic liquids used in this study were composed of the following ions: 1-ethyl-3-methylimidazolium, 1-butyl-3-methylimidazolium, acetate, formate and lactate (Scheme 1). The results obtained from the measurements using the volumetric method were checked using gravimetric control experiments.

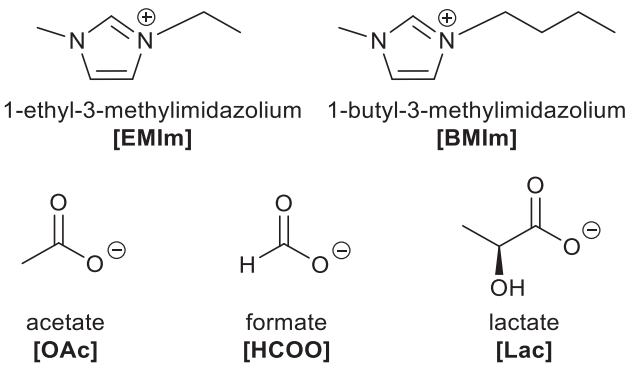

Scheme 1. Cations and anions in the six selected ILs for water vapor sorption.

2. Experimental section

2.1. Materials

Commercial chemicals were used without further purification. Anion exchange resin Amberlyst® A26 (OH^--form) was purchased from Acros Organics, *(S)*–lactic acid was purchased as a 90 % solution in water from Caesar & Loretz (ee = 96.96 %), 1-ethyl-3-methylimidazolium bromide ([EMIm]Br, ≥ 97 %) and 1-butyl-3-methylimidazolium chloride ([BMIm]Cl, ≥ 98 %) were purchased from Sigma Aldrich. Water with a residual conductivity of 0.05 µS/cm at 25 °C was obtained from a MILLIPORE Synergy® water purification system.

2.2. Synthesis of ionic liquids

All ionic liquids were synthesized using the anion exchange method described by Alcalde *et al.* [36]. In short, a glass column was filled with anion exchange resin Amberlyst® A-26 (OH^-–form) and consequently, the OH^--ions were exchanged with the desired anion by slowly passing a 1 % solution of ammonium acetate/formate in water or a 1 % solution of *(S)*-lactic acid in water:methanol (1:1 v:v) through the column, until the pH of the eluate reached the same value as the base solution (pH = 6 for ammonium acetate/formate, pH = 4 for *(S)*-lactic acid). Subsequently, a 1 % solution of [EMIm]Br or [BMIm]Cl in water was slowly passed through the column to exchange the halide with the desired carboxylate anion. Afterwards, the solvent was removed by rotary evaporation and the ionic liquids dried at 60 °C under vacuum for at least 16 h. All anion-exchanged ionic liquids were received in nearly quantitative yields. The purity of the ILs was established by ^{1}H and ^{13}C NMR (Section 3, SI) and by anion chromatography (Section 4, SI), the water content was determined after drying by Karl Fischer titration.

2.3. Analytical methods

^{1}H and ^{13}C NMR spectra were recorded either with a BRUKER Avance III–600 or a BRUKER Avance DRX–500 at 297 K and are referenced to the residual solvent signal relative to TMS ($CDCl_3$ ^{1}H NMR 7.26 ppm, ^{13}C NMR 77.36 ppm; D_2O ^{1}H NMR 4.79 ppm). Diffusion measurements have been conducted on a BRUKER Avance III–600 with a gradient field of up to 47 G/cm, a diffusion time of 310 ms and a gradient pulse duration of 2 ms.

Anion exchange chromatography was carried out using a THERMO SCIENTIFIC Dionex ICS 1100 chromatograph with the anion exchange

resin IonPac® AS22. The background conductivity of the eluent was suppressed using a self-regenerating suppressor AERS500.

Thermogravimetric analysis (TGA) was conducted with a NETZSCH TG 209 F3 Tarsus, applying a heating rate of 5 K/min until 600 °C under nitrogen gas.

Coulometric Karl-Fischer titration was performed with an ECH/ANALYTIK JENA AQUA 40.00 Karl Fischer titrator via direct injection into the cell.

Volumetric water sorption isotherms were determined using a QUANTACHROME VStar 4 at 293 K. Prior to the measurements, the samples were activated for at least 3 h at 60 °C using a QUANTACHROME Flovac Degasser. For each point, the equilibrium conditions were as follows: the equilibrium points number was set to 10 points with an interval time of 60–90 s and a sorption rate limit of 0.005 Torr/min at low relative pressures (p/p_0 = 0.001 – 0.6) and 0.01 Torr/min at high relative pressures (p/p_0 = 0.7 – 0.9) (see Supporting Information Section 6 for details). The error of volumetric water sorption measurements is in the range of 2 %. Additional water sorption experiments were conducted on a QUANTACHROME Autosorb-iQ-MP at 293 K with the same degassing protocol prior to the measurement. For the gravimetric control experiments, temperature and relative humidity were checked using a VWR hygro-/thermometer TH300.

3. Results and discussion

3.1. IL synthesis and characterization

The synthesis of the ILs was conducted by the anion exchange method starting with the 1-alkyl-3-methylimidazolium halide as described before [36]. In short, a solution of an imidazolium halide was passed over the anion exchange resin loaded with the desired anion (Scheme 2).

After drying of the IL, the ^{1}H and ^{13}C NMR spectra (Supporting Information, Figs. S3–S14) show impurities only for the ILs with the lactate anion, where a few additional peaks were present. These could be traced to the used slightly impure *(S)*-lactic acid, which also exhibited these same additional peaks. Additionally, the anion purity of the ILs was determined by ion chromatography and was in all cases above 98 %. All anion chromatograms can be found in the Supporting Information (Figs. S15–S20).

The thermal stability of the ILs was examined with TGA at a heating rate of 5 K/min until 600 °C. The TGA diagrams (SI, Fig. S21) show that the thermal stability greatly depends on the type of anion. While the $[OAc]^-$ and $[HCOO]^-$ based ILs decompose at around 210 °C, those bearing the $[Lac]^-$ anion are slightly more thermally stable, up to around 230 °C. This is caused by the additional hydroxyl-group in the [Lac] anion creating a stronger anion-cation-interaction [12]. However, as already explained in the introduction, the thermal stability of ILs can only be approximated by TGA scans with conventional heating rates of 5 K min^{-1} [18–19]. It is not clear if these lower thermal stabilities arise from the formation of *N*-heterocyclic carbenes (NHC). While the formation of NHCs could not be confirmed experimentally yet and theoretical studies deny the possibility of NHC formation, carboxylate-based ILs could be successfully used in otherwise NHC catalyzed reactions, which suggest these ionic liquids to be "proto-carbenes" [37–38].

The water content of the ionic liquids was determined by coulometric Karl-Fischer titration between 1.0 and 4.5 wt%.

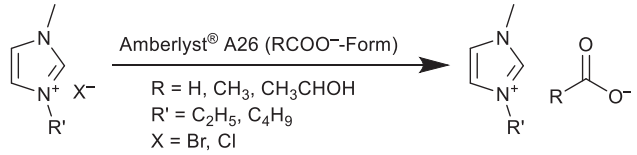

Scheme 2. Reaction scheme for the anion exchange process yielding the imidazolium carboxylate ILs.

3.2. Volumetric water sorption measurements at given amount

Water sorption isotherms were measured at 20 °C for all six IL samples and are depicted in Fig. 1.

All six ionic liquids show a very high water uptake, exceeding 1000 mg/g. It is evident that neither of the ILs reaches saturation at 0.9 bar under the given experimental conditions. All isotherms exhibit a high positive, apparently even increasing slope and are far from levelling off at 0.9 bar. This indicates an absorption curve far from saturation, which will be reached only at higher pressures. The degree of hysteresis between absorption and desorption varies.

For the ILs with the [EMIm] cation (Fig. 1a), [EMIm][Lac] shows the highest water uptake with 1570 mg/g, followed by [EMIm][OAc] with 1470 mg/g and [EMIm][HCOO] with 1280 mg/g (Table 1). For the [BMIm] cation ILs (Fig. 1b) [BMIm][OAc] shows the highest water uptake with 1830 mg/g, followed by [BMIm][Lac] with 1420 mg/g and [BMIm][HCOO] with 1210 mg/g (Table 1). The ordering will not be discussed in detail here based on the later apparent kinetic effects (see below). We only note that additional hydrophilic groups in the lactate anion were expected to increase the IL-anion-cation interaction and hence decrease the ion-water interaction [12]. But it is also visible that [EMIm][Lac] only has a

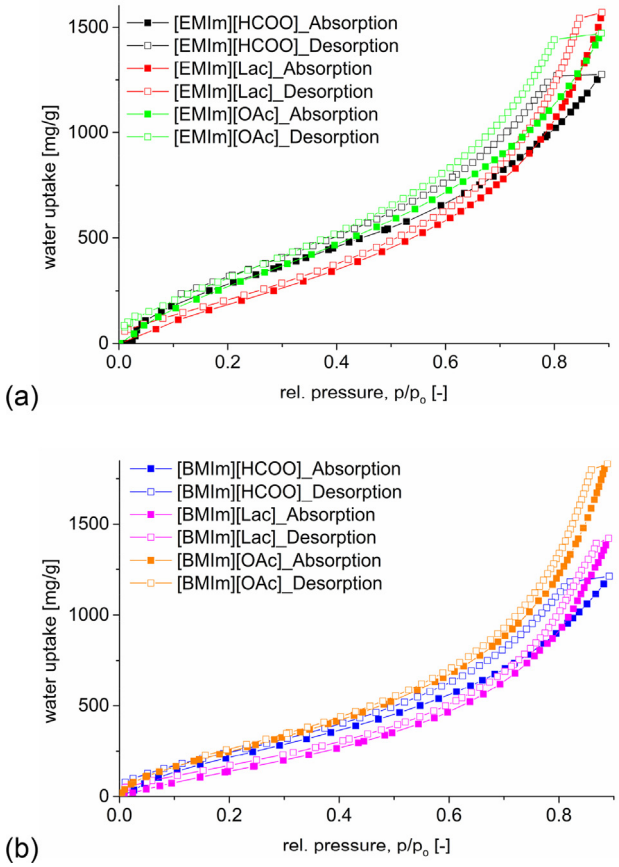

Fig. 1. Water sorption isotherms of the ionic liquids (a) with $[EMIm]^+$ cations and (b) with $[BMIm]^+$ cation, measured at 20 °C in the relative pressure range of p/p_0 = 0 – 0.9; sample mass was between 10 and 35 mg. Filled symbols represent absorption, empty one's desorption. For the overlay of the isotherms for the same anion see Fig. S23, SI.

Table 1
Results of volumetric water sorption experiments summarized in comparison to previously determined sorption capacities using the gravimetric method.

Ionic liquid	Method	Conditions	Sample amount [mg]	Water uptake [mg/g]	Ref.
[EMIm][OAc]	gravimetric	25.3 °C, 35.3 % RH		738[a]	[11]
	volumetric	20 °C, p/p_0 = 0.35	23.6	424	This work
	volumetric	20 °C, p/p_0 = 0.9	23.6	1470	This work
[BMIm][OAc]	gravimetric	21.7 °C, 26.7 % RH		242	[39]
	gravimetric	25.3 °C, 35.3 % RH		251[a]	[11]
	gravimetric	23 °C, 52 % RH		242[b]	[23]
	volumetric	20 °C, p/p_0 = 0.27	10.4	314	This work
	volumetric	20 °C, p/p_0 = 0.35	10.4	369	This work
	volumetric	20 °C, p/p_0 = 0.54	10.4	584	This work
	volumetric	20 °C, p/p_0 = 0.9	10.4	1830	This work
[EMIm][HCOO]	volumetric	20 °C, p/p_0 = 0.9	34.9	1280	This work
[BMIm][HCOO]	volumetric	20 °C, p/p_0 = 0.9	24.1	1210	This work
[EMIm][Lac]	volumetric	20 °C, p/p_0 = 0.9	32.3	1570	This work
[BMIm][Lac]	volumetric	20 °C, p/p_0 = 0.9	16.0	1420	This work
[EMIm][$MeSO_3$]	volumetric	25 °C, p/p_0 = 0.9		1250-1500[c]	[34,35]

[a] Extrapolated from 40 h measurement.
[b] Extrapolated from 3 h measurement.
[c] Estimated from sorption isotherm plot.

higher water uptake in the high relative pressure ranges starting from p/p_0 = 0.75. When zooming into the low relative pressure range for the [EMIm] ILs (Fig. S24, SI) it is visible that [EMIm][HCOO] displays a sudden increase in the water sorption capacity, a behavior no other IL shows. A possible explanation could be the fact that [EMIm][HCOO] is the only ionic liquid which is not liquid at room temperature. As a result, water vapor can barely be absorbed into the IL bulk. Only after some water has already been absorbed, the now IL-water mixture starts to become liquid, hence enabling the water absorption.

At first sight, for the same anion, the total water uptake can be changed significantly with only small variations in the cation from [EMIm] to [BMIm]. For [OAc] the uptake increases by about 260 mg/g while for [Lac] it decreases by about 150 mg/g when replacing the [EMIm] by the [BMIm] cation (Fig. S22b,c). The opposite effect was at first puzzling and especially the higher uptake of [BMIm][OAc] vs. [EMIm][OAc] appeared counterintuitive, since longer alkyl chains should make the IL more hydrophobic and thereby decrease the water uptake capacity [23]. The molecular volume V_m, defined as the sum of the ionic volumes V_{ion}, is another option to predict physical properties of ionic liquids. The ionic volumes have been determined before as 0.156 nm^3 for $[EMIm]^+$, 0.196 nm^3 for $[BMIm]^+$, 0.049 nm^3 for $[OAc]^-$, 0.064 nm^3 for $[HCOO]^-$ and 0.101 nm^3 for $[Lac]^-$ [13,39]. It could be shown that the molar concentration of ionic liquids decreases with increasing molecular volume, hence the ionic liquid with lowest molecular volume should have the highest molar concentration, from which one could assume that it might have the highest water uptake. In this case [EMIm][OAc] would be predicted to have the highest water uptake and [BMIm][Lac] the lowest. However, this does not coincide with the experimental data. Again, due to the kinetic artefact (see below) we will not discuss this trend any further.

Water uptake has previously only been reported for the two [OAc]-based ILs with the gravimetric method at static conditions (Table 1) [11,23,40]. For comparison, relative humidity and relative pressure are interchangeable by the equation $\%RH = p/p_0 \cdot 100\%$. When comparing our results to previously reported work, strong deviations in water uptake became evident. Furthermore, already the literature-reported water uptake capacities for [BMIm][OAc] were not consistent, as the ionic liquid showed nearly the same water uptake (around 245 mg/g), independent of temperature and relative humidity [11,23,39]. These results will be discussed further in the following.

3.3. Mass dependence

As neither of the ILs reaches a saturation in water uptake at p/p_0 = 0.9 the possibility of a kinetic effect emerged. The diffusion of water into the bulk IL decreases with increasing viscosity, hence it should be slower in [BMIm] ILs since the viscosity increases with the alkyl chain length [9,17]. On the other hand, longer alkyl groups on the cation create additional "free volume" in the IL, increasing the mobility of water in the bulk [25,41].

When reproducing the sorption measurements, it became evident that the results strongly depend on the used amount of the IL. Initial typical sample masses for the absorption isotherms in Fig. 1 ranged from 10 to 35 mg. The water sorption isotherms for [BMIm][OAc] gave an inversely proportional uptake with the sample amount, that is the maximum uptake decreased almost linearly with increasing sample mass (Fig. 2). It is evident from Fig. 2 that the determination of IL water sorption by volumetric measurements will underestimate the water sorption capacity due to the slow uptake for bulk samples and the still too short equilibration times (see below) in automatic volumetric gas and vapor sorption analyzers.

The water sorption capacity of [BMIm][OAc] ranged from 2100 mg/g for 6.67 mg of sample to 900 mg/g for 64.14 mg of IL sample (Table 2). Extrapolation of the water uptake to very small IL amounts with negligible kinetic hindrance than gives an equilibrium water uptake capacity of over 2100 mg/g(IL) at p/p_0 = 0.9. To the best of our knowledge, we are not aware that a mass-dependent water uptake in ILs has been reported before. Sorption isotherm measurement assume a thermodynamic equilibrium at each data point. It is only known that the transport properties of ionic liquids change with the scale of the experiment. Berrod *et al.* could show that for [BMIm][NTf_2] ([NTf_2] = bis(trifluormethyl sulfonyl)imide, bistriflimide) the self-diffusion coefficient of the cation is about six times smaller when measured on the ns–ms/nm-μm scale (using pulsed-field-gradient-NMR techniques), compared to the results obtained on the ps–ns/0.1–10 nm scale (using quasi-elastic neutron scattering, QENS-experiments) [42]. In the same study it was found by dynamic light scattering (DLS) experiments on latex nanoparticles inside the IL, that ionic liquids show a similar behavior as it is observed in micelles, arguing in favor of micelle-like structure of ILs. This self-organization creates spatial heterogeneities, affecting the mean IL dynamics. Burankowa *et al.* could prove the same behavior regarding the diffusion coefficients

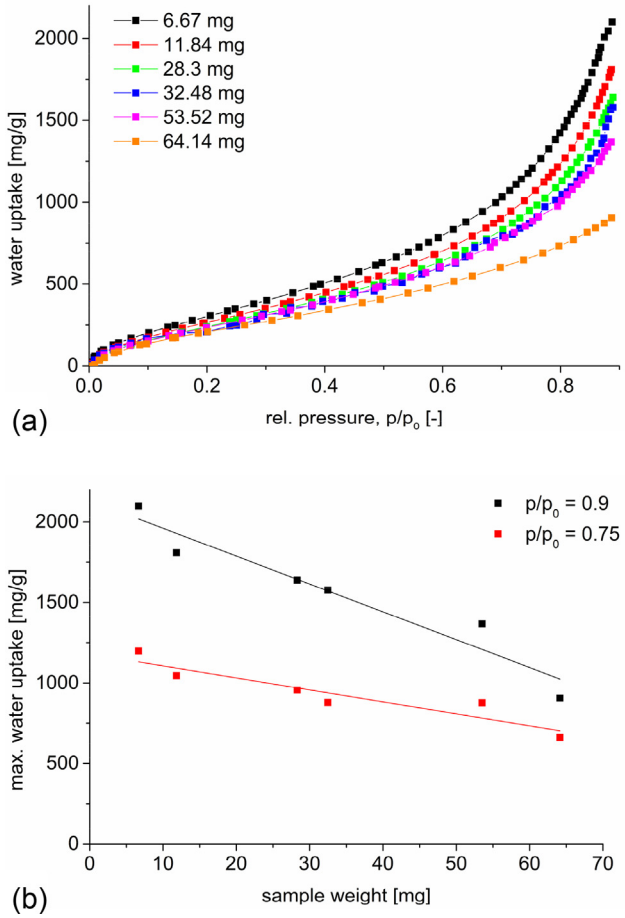

Fig. 2. (a) Water sorption isotherms for six different sample masses of [BMIm][OAc], measured at 20 °C in the relative pressure range of p/p_0 = 0 – 0.9. For clarity, only the absorption branch is shown. (b) Mass dependence of the maximum water uptake at p/p_0 = 0.9 and 0.75 of [BMIm][OAc]; the trendlines are a guide to the eye.

Table 2
Volumetric water sorption capacities for different amounts of [BMIm][OAc].

Sample amount [mg]	H_2O uptake at p/p_0 = 0.9 [mg/g]	H_2O uptake at p/p_0 = 0.75 [mg/g]	H_2O uptake at p/p_0 = 0.3 [mg/g]
6.67	2099	1198	400
11.84	1809	1046	352
28.30	1639	956	319
32.48	1577	879	315
53.52	1367	877	305
64.14	906	662	278

also using QENS-experiments for the ionic liquid [BuPy][NTf_2] ([BuPy] = *N*-butylpyridinium) [43]. Here, our results indicate a rather slow water sorption process, which is slower than equilibration times during the measurements so that the water uptake is strongly influenced by the time given during the measurement. The measurement was carried out with the longest possible equilibration time, that is up to 900 s on each pressure data point with a pressure-change rate limit of 0.001 to 0.01 Torr/min (see Supporting Information Section 6 for details). The rate of the water sorption process for (I) adsorption of water at the IL surface, (II) absorption of water into the IL by diffusion may thus depend on the available surface area relative to the sample amount. A larger relative surface area, that is a smaller sample amount should result in a faster water uptake and vice versa.

To check this conclusion, we conducted another set of water-sorption experiments using a QUANTACHROME iQ volumetric sorption device. At the iQ device, it was possible to stir the IL during the measurement with a magnetic stirrer in the sample tube and thereby increase the surface area for the given sample amount. The resulting isotherms and water uptake in Fig. 3 demonstrate that under stirring the water sorption capacity increases. At a relative pressure of p/p_0 = 0.8 the uptake is 930 mg/g when the sample is stirred, without stirring the uptake is only 785 mg/g. The increase in water uptake is 145 mg/g simply by stirring the sample, that is providing a larger surface area to accelerate the water uptake. This supports the assumption of a kinetically controlled water vapor sorption process. The stirring speed was put to the slowest possible setting (at around 50 rpm), because higher stirring speeds caused interference with the pressure measurement (especially during crucial steps as cell volume measurement). Hence, faster stirring was not possible. But it would be expected that faster stirring would increase the sorption capacity at any given point, until the equilibrium water uptake is reached.

3.4. Gravimetric control tests

Due to the mass-dependence of the water uptake from the volumetric method we also conducted gravimetric control tests which allowed for an extended water uptake time of up to 90 days at a preset humidity. A desiccator containing a dish with a saturated sodium chloride solution was used to give a stable relative humidity (RH) of around 75.5 % [44], in which the IL samples were stored. A schematic illustration of the setup is shown in Fig. 4. These experiments have been exemplarily conducted for [BMIm][OAc].

For the first experiment, four tubes with the same diameter (6 mm) were filled with different amounts of [BMIm][OAc], for the second experiment, the same amount of the IL (around 85 mg) was filled into tubes with varying diameters (4, 6, 8 and 10 mm, Table 3), corresponding to increasing surface areas of 12.6, 28.3, 50.3 and 78.5 mm^2, respectively. After placing these tubes in the desiccator with the saturated NaCl-solution, the increase in mass was checked regularly (every two days) using an analytical balance (the maximum error is given by the error of the balance and does not exceed 0.2 %). The resulting absorption

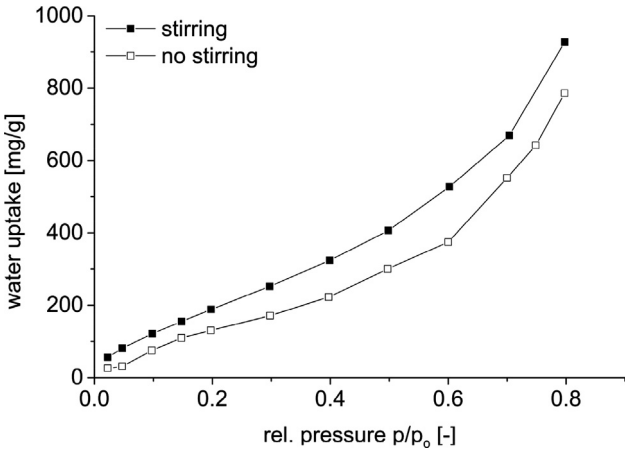

Fig. 3. Water absorption isotherms of [BMIm][OAc] using a QUANTACHROME iQ in a relative pressure range of p/p_0 = 0 – 0.8. Filled symbols represent the measurements with a stirred sample, empty symbols represent the measurement without stirring. Both measurements have been carried out with the exact same sample (sample amount 130 mg). During the measurement without stirring, the stirring bar was still left inside the sample tube to ensure the same conditions. Note that the water uptake values cannot be compared to the values in Fig. 2 since the sample tube gave rise to a different IL surface area and thickness (see below).

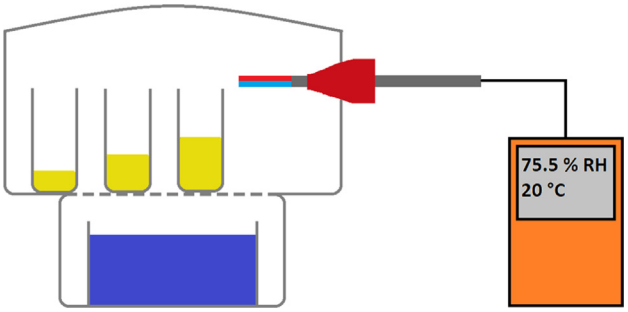

Fig. 4. Schematic illustration of the setup for gravimetric water vapor sorption experiments. A desiccator containing a saturated NaCl-solution (blue) provided an atmosphere with stable relative humidity in which the IL samples (yellow) were kept for 90 days. Temperature and relative humidity were monitored using a connected hygro-/thermometer. (For interpretation of the references to colour in this figure legend, the reader is referred to the web version of this article.)

curves are plotted in Fig. 5a. As can be clearly seen, the ionic liquid takes up water continuously with a decreasing sorption rate when the maximum uptake is approached and all samples converge to a water uptake of nearly exactly 1040 mg/g as should roughly be expected from the extrapolation of the volumetric uptake at $p/p_0 = 0.75$ for the different IL masses to very small IL amounts with negligible kinetic hindrance (Fig. 2b). It can also be clearly seen, that the time to reach the maximum water uptake increases with increasing amount of IL at equal surface area. While the sample with the least amount of [BMIm][OAc] reaches equilibrium after around 12 days, it takes the sample with the highest amount 42 days to reach the same water uptake from air (Fig. 5c). This comparison at equal surface area clearly indicates that the process of water sorption is kinetically controlled by diffusion from the surface into bulk of the IL. A kinetically controlled diffusion process is further supported by the faster water uptake for equal amounts of IL with increasing surface area (Fig. 5b). A limiting factor during the water vapor sorption is the ratio of the surface area at the gas–liquid-interface to the mass of the ionic liquid. The time until the samples reach equilibrium is inversely exponentially proportional to the surface area and linearly proportional to the amount of the IL (Fig. 5c). With a surface area of 78.5 mm^2 it takes about 14 days and for the same amount of IL but a surface area of only 12.6 mm^2 more than 56 days are needed. The results are summarized in Table 3.

At a water uptake of 1000 mg/g, the mole fraction of water x_w reaches a value of $x_w = 0.9$. It could be shown previously for [BMIm][OAc] that at this mole fraction, every anion is coordinated by 5.61 molecules of water, which corresponds to the coordination number of acetate ions in aqueous solution [26]. Even at such high water contents ionic liquids still behave as the continuous phase [27].

From Fig. 5a and b the difference in water uptake is visible until all samples have reached equilibrium in water absorption. The water uptake curves over time level-off slowly towards the equilibrium uptake. Thus, it is not evident that an increase in water concentration in the IL enhances the rate of water uptake from the surface into the bulk. If the imidazolium alkyl chains are preferentially oriented to the vapor phase [9], then the surface adsorbed water must overcome this hydrophobic barrier. The water-clusters inside the ionic liquid, which form at higher water concentrations [25–26] would have little effect on the rate-limiting surface-to-bulk transition.

The absorption can be described by a pseudo second order absorption kinetics as given in Eq. (1)

$$q_t = \frac{t}{1/(k * q_e^2) + t/q_e} \quad (1)$$

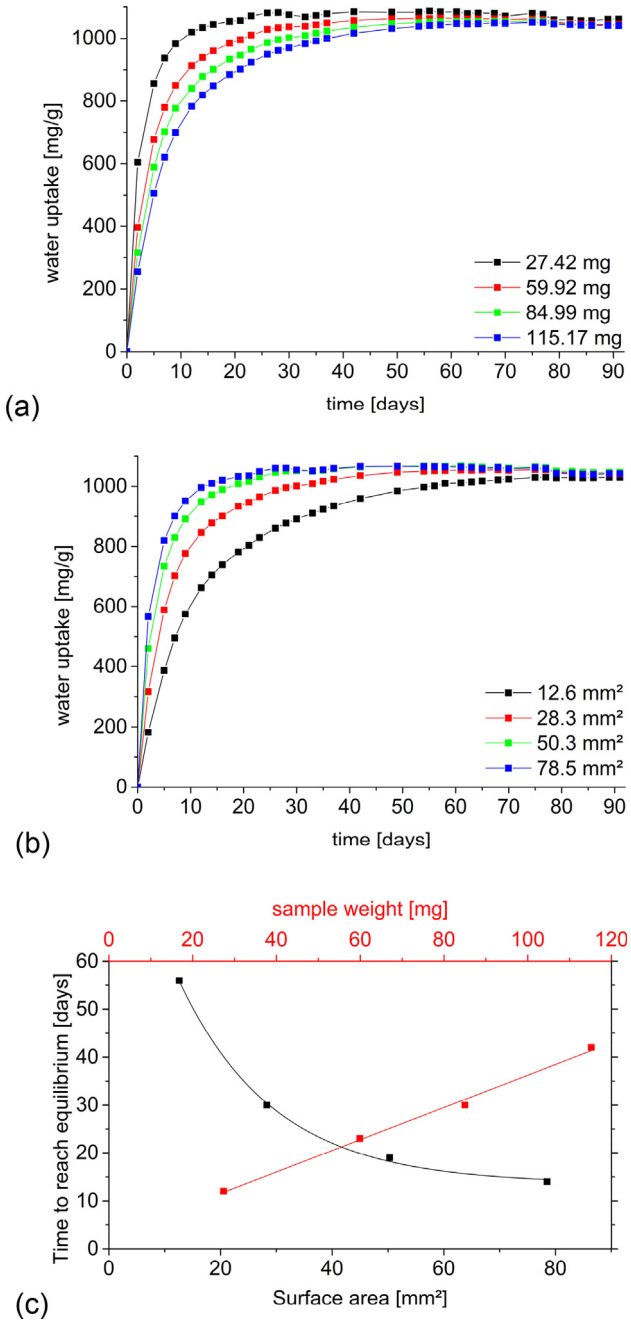

Fig. 5. Gravimetrically determined water absorption curves at 75.5 % RH of (a) different amounts of [BMIm][OAc] in tubes with 6 mm diameter and (b) of the same amount of [BMIm][OAc] (85 mg) with different surface area (due to tubes with different diameters). (c) Time to reach the equilibrium of water sorption for [BMIm][OAc] in dependence of the surface area at the same (fixed) sample weight (black) and in dependence of the sample weight at the same surface area (red). For comparison, the time to reach equilibrium has been determined as the amount of days it took each sample to surpass a water uptake of 1000 mg/g, the trendline is a guide to the eye. (For interpretation of the references to colour in this figure legend, the reader is referred to the web version of this article.)

where q_t [mg/g] is the absorption capacity at any given time t [days], q_e [mg/g] is the absorption capacity at equilibrium and k [g/(mg·days)] represents the pseudo second order rate constant. This has been exemplarily conducted for the samples containing the same amount of IL with different surface areas (Fig. 5b). The pseudo second order absorption kinetics proved to be an adequate fitting equation giving a correlated $R^2 > 0.98$ in all cases, the resulting curves are shown in Fig. S25 (Supporting Information). In accor-

Table 3
Time to reach equilibrium of the samples used for gravimetric water sorption experiments in dependence of the exposed surface area at the liquid–gas interface and the amount of [BMIm][OAc].

Tube diameter [mm] [a]	Surface area [mm²]	Amount IL [mg]	Time to equilibrium [d] [b]
4	12.6	83.6	56
6	28.3	85.0	30
8	50.3	82.8	19
10	78.5	83.3	14
6	28.3	27.4	12
6	28.3	59.9	23
6	28.3	85.0	30
6	28.3	115.2	42

[a] Exact diameters were: 3.96, 5.96, 7.95 and 9.94 mm.
[b] Time to pass a water uptake of 1000 mg/g based on the converged water uptake values of 1040 mg/g in Fig. 5a,b.

dance to the other results, the apparent rate constant of absorption increases with increasing surface area, supporting the assumption of faster absorption kinetics for thinner IL-films. For the given data, the absorption rate constants are $9.5{\cdot}10^{-5}$, $2.2{\cdot}10^{-4}$, $3.9{\cdot}10^{-4}$ and $6.0{\cdot}10^{-4}$ g/(mg·days) for surface areas of 12.6, 28.3, 50.3 and 78.5 mm², respectively.

In a control experiment the tubes of different diameters were charged with different amounts of [BMIm][OAc] to reach the same mass-specific surface area. The resulting absorption curves in Fig. 6 show nearly the same time-dependent water uptake in the first 22 days. These findings verify the assumption that the water vapor sorption in ionic liquids is a strongly kinetically controlled diffusion process for the absorption of water from the surface into the bulk IL. Xie *et al.* reported a similar behavior for the CO_2 sorption of ionic liquids immobilized on titanium dioxide. It was shown, that the equilibrium time for CO_2 uptake increased with increasing film thickness of the IL on the support in the nanoscale regime with an up to 10 times longer equilibration time for thicker IL-films [45]. Noteworthy also the gas-dehydration work of Radakovisch *et al.* [34–35] applied the IL [EMIm][$MeSO_3$] as a thin layer ionic-liquid phase coated on silica gel [46–47] because of the inherent short diffusion paths.

Consequently, the fastest absorption rate should be reached when the ionic liquid is applied as a thin film, thus maximizing the mass-based surface area. At the same time, for the determination of the water vapor uptake of ILs, conventional sorption methods must consider the slow water diffusion into the IL, that is a considerably longer time to reach thermodynamic equilibrium than for other materials.

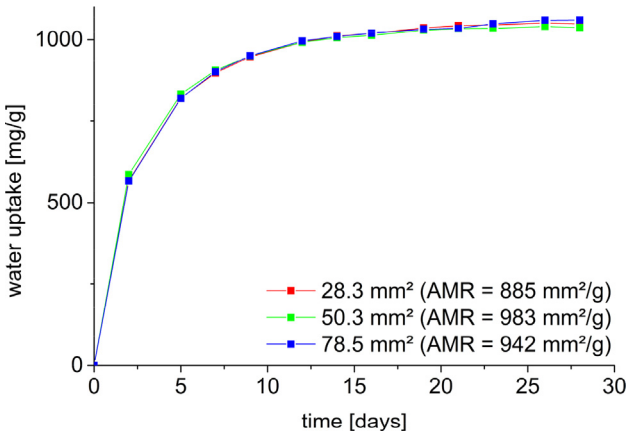

Fig. 6. Gravimetrically determined absorption curves at around 75.5 % RH of different amounts of [BMIm][OAc] in vials with different diameters and thereby a similar initial mass-specific surface area (area-mass relation, AMR).

NMR techniques can be used to determine diffusion coefficients using gradient techniques according to the Stejskal-Tanner equation (2) and this has already been performed for the mixture of [EMIm][OAc] with water [12].

$$\frac{I}{I_0} = \exp(-\gamma^2 g^2 \delta^2 \left(\Delta - \frac{\delta}{3}\right) D) \quad (2)$$

where I/I_0 is the NMR signal ratio with and without gradient field, γ is the gyromagnetic ratio of ^1H, g is the gradient field strength, δ the gradient pulse duration, Δ the diffusion time between pulses and D is the sought-after diffusion coefficient. The experiment has been conducted for a sample of [BMIm][OAc] with a water content of 9 wt-% (as determined by Karl-Fischer-Titration) at 298 K. It should be noted, however, that the ionic liquid and water were premixed and that the results do not represent the diffusion of water from the gas into the liquid phase. For the given conditions the following diffusion coefficients were determined: for water $(1.4 \pm 0.1){\cdot}10^{-10}$ m²/s, for the [OAc] anion $(5.0 \pm 0.4){\cdot}10^{-11}$ m²/s and for the [BMIm] cation $(3.8 \pm 0.5){\cdot}10^{-11}$ m²/s. These results are in accordance to previous findings that water diffuses considerably faster in IL/water mixtures than the ions [12]. Together with our other results, this supports the assumption that the diffusion of water from the adsorbed surface phase into the liquid IL phase is the rate limiting step, which also explains faster absorption kinetics when the ionic liquid is applied as a thin film.

To check the validity of the results from [BMIm][OAc] for other hydrophilic ionic liquids, we conducted another gravimetric sorption experiment with [EMIm][OAc] using different amounts of the IL in tubes with same diameter at RH = 75.5 %. In the same manner as for [BMIm][OAc], the sample with the highest ratio of gas–liquid-interface to volume (i.e. the sample with the lowest amount of ionic liquid) was the one which reached equilibrium the fastest. The time to reach equilibrium (i.e. a water sorption capacity of 1350 mg/g) ranged from two weeks for the lowest sample amount of 52 mg to six weeks for the highest one of 197 mg (Fig. S26, Supporting Information).

4. Conclusions

In this study we report complete water sorption isotherms for six pristine hydrophilic ionic liquids using the volumetric method over the relative pressure range of $p/p_0 = 0 – 0.9$ for the first time. All ionic liquids show a steady and high water uptake with a small hysteresis between absorption and desorption. However, repeated measurements with different amounts of IL showed that the g(water)/g(IL) uptake strongly deviates with the amount of the IL used for the sorption experiment. Further volumetric measurements with the example [BMIm][OAc] showed that the maximum g/g water uptake decreases with increasing amount of the IL when the surface area stays similar. These results indicate that the process of water sorption is rather slow and strongly dependent by diffusion of the water from the IL surface into the bulk. Additional water sorption experiments, in which it was possible to stir the liquid during the sorption process, also indicated a slow and diffusion-driven absorption process. Therefore, automatic volumetric water sorption studies are only meaningful with different amounts of sample so as to extrapolate the uptake to very small IL amounts with negligible kinetic hindrance. Furthermore, the water sorption capacities of different ionic liquids are only comparable if the same amount of sample is used for every sorption experiment, or more precisely if the ratio of exposed surface area to the volume of the sample is the same in all cases.

Gravimetric control experiments were conducted with [BMIm][OAc] using a saturated NaCl-solution inside a desiccator, creating a stable relative humidity (RH) of around 75.5 %, and confirmed the assumption of a diffusion driven sorption process. While all samples reached an equilibrium maximum water uptake of circa 1040 mg/g at this RH, the time to reach this equilibrium increased linearly with the amount of the IL and was inversely exponentially proportional to the surface area at the gas–liquid-interface of the IL. Thereby, results show a strong dependence of the sorption time from the initial ratio of the surface area to the mass of the ionic liquid. Gravimetric water sorption of samples with different amount of IL but with the same mass-specific surface area lead to the same time-dependent absorption curves, further confirming the results. As already shown for CO_2 sorption, also for water sorption the fastest sorption rates will be achieved when the IL is used as a thin film as in supported ionic liquid phases.

For future experiments, the role of the enantiomer vs. racemic mixture in the case of lactate-based ionic liquids seem worth to be studied, to see if different structural arrangements in the IL have an effect on overall water sorption properties.

CRediT authorship contribution statement

Alex Spieß: Conceptualization, Methodology, Formal analysis, Investigation, Writing – original draft, Writing – review & editing. **Philipp Brandt:** Investigation. **Alexa Schmitz:** Investigation. **Christoph Janiak:** Supervision, Project administration, Funding acquisition, Writing – review & editing.

Declaration of Competing Interest

The authors declare that they have no known competing financial interests or personal relationships that could have appeared to influence the work reported in this paper.

Acknowledgement

The authors thank the Federal German Ministry of Education and Research (BMBF) through the project Optimat, grant 03SF0492C and the German Research Foundation (DFG) in the framework of the priority program SPP 1708, grant JA 466/31-2 for financial support.

Appendix A. Supplementary material

Supplementary data to this article can be found online at https://doi.org/10.1016/j.molliq.2021.118023.

References

[1] Y. Zhou, M. Antonietti, Preparation of Highly Ordered Monolithic Super-Microporous Lamellar Silica with a Room-Temperature Ionic Liquid as Template via the Nanocasting Technique, Adv. Mater. 15 (17) (2003) 1452–1455, https://doi.org/10.1002/adma.200305265.
[2] P. Wasserscheid, W. Keim, Ionic Liquids—New "Solutions" for Transition Metal Catalysis, Angew. Chem. Int. Ed. 39 (2000) 3772–3789, https://doi.org/10.1002/1521-3773(20001103)39:21<3772::AID-ANIE3772>3.0.CO;2-5.
[3] M.G. Freire, C.M.S.S. Neves, P.J. Carvalho, R.L. Gardas, A.M. Fernandes, I.M. Marrucho, L.M.N.B.F. Santos, J.A.P. Coutinho, Mutual solubilities of water and hydrophobic ionic liquids, J. Phys. Chem. B 111 (45) (2007) 13082–13089, https://doi.org/10.1021/jp076271e.
[4] T. Welton, Room-Temperature Ionic Liquids. Solvents for Synthesis and Catalysis, Chem. Rev. 99 (8) (1999) 2071–2084, https://doi.org/10.1021/cr980032t.
[5] J.J. Beaulieu, J.L. Tank, M. Kopacz, Sorption of imidazolium-based ionic liquids to aquatic sediments, Chemosphere 70 (7) (2008) 1320–1328, https://doi.org/10.1016/j.chemosphere.2007.07.046.
[6] R.S. Anaredy, A.J. Lucio, S.K. Shaw, Adventitious Water Sorption in a Hydrophilic and a Hydrophobic Ionic Liquid, ACS Omega 1 (2016) 407–416, https://doi.org/10.1021/acsomega.6b00104.
[7] K.R. Seddon, A. Stark, M.-J. Torres, Influence of chloride, water, and organic solvents on the physical properties of ionic liquids, Pure Appl. Chem. 72 (2000) 2275–2287, https://doi.org/10.1351/pac200072122275.
[8] A. Dahi, K. Fatyeyeva, C. Chappey, D. Langevin, S.P. Rogalsky, O.P. Tarasyuk, S. Marais, Water sorption properties of room-temperature ionic liquids over the whole range of water activity and molecular states of water in these media, RSC Adv. 5 (94) (2015) 76927–76938, https://doi.org/10.1039/C5RA14066H.
[9] F. Di Francesco, N. Calisi, M. Creatini, B. Melai, P. Salvo, C. Chiappe, Water sorption by anhydrous ionic liquids, Green Chem. 13 (2011) 1712–1717, https://doi.org/10.1039/c1gc15080d.
[10] J.P. Hallett, T. Welton, Room-temperature ionic liquids: solvents for synthesis and catalysis. 2, Chem. Rev. 111 (5) (2011) 3508–3576, https://doi.org/10.1021/cr1003248.
[11] Y.u. Chen, Y. Cao, T. Mu, A New Application of Acetate-Based Ionic Liquids: Potential Usage as Drying Materials, Chem. Eng. Technol. 37 (3) (2014) 527–534, https://doi.org/10.1002/ceat.201300583.
[12] T. Brünig, M. Maurer, R. Pietschnig, Sorbent Properties of Halide-Free Ionic Liquids for Water and CO_2 Perfusion, ACS Sustainable Chem. Eng. 5 (8) (2017) 7228–7239, https://doi.org/10.1021/acssuschemeng.7b01468.
[13] T. Brünig, K. Krekić, C. Bruhn, R. Pietschnig, Calorimetric Studies and Structural Aspects of Ionic Liquids in Designing Sorption Materials for Thermal Energy Storage, Chem. Eur. J. 22 (45) (2016) 16200–16212, https://doi.org/10.1002/chem.201602723.
[14] B. Brandt, Korrosionsverhalten ausgewählter Werkstoffe in Lithiumbromid-Lösung für den Anwendungsfall Absorptionskältemaschinen, Mater. Corros. 55 (7) (2004) 536–542, https://doi.org/10.1002/maco.200303766.
[15] M. Bücherl, F. Hardock, E. Kaiser, A. Netsch, K. Schaber, Density, Viscosity, and Vapor-Liquid Equilibrium of the Ternary System Water-1-Ethyl-3-methylimidazolium Acetate-1-Ethyl-3-Methylimidazolium Trifluoromethanesulfonate, J. Chem. Eng. Data 62 (2) (2017) 720–728, https://doi.org/10.1021/acs.jced.6b00801.
[16] N. Merkel, M. Bücherl, M. Zimmermann, V. Wagner, K. Schaber, Operation of an absorption heat transformer using water/ionic liquid as working fluid, Appl. Therm. Eng. 131 (2018) 370–380, https://doi.org/10.1016/j.applthermaleng.2017.11.147.
[17] J.G. Huddleston, A.E. Visser, W.M. Reichert, H.D. Willauer, G.A. Broker, R.D. Rogers, Characterization and comparison of hydrophilic and hydrophobic room temperature ionic liquids incorporating the imidazolium cation, Green Chem. 3 (2001) 156–164, https://doi.org/10.1039/b103275p.
[18] M. Kosmulski, J. Gustafsson, J.B. Rosenholm, Thermal stability of low temperature ionic liquids revisited, Thermochim. Acta 412 (1-2) (2004) 47–53, https://doi.org/10.1016/j.tca.2003.08.022.
[19] Y. Cao, T. Mu, Comprehensive Investigation on the Thermal Stability of 66 Ionic Liquids by Thermogravimetric Analysis, Ind. Eng. Chem. Res. 53 (20) (2014) 8651–8664, https://doi.org/10.1021/ie5009597.
[20] N. Merkel, C. Weber, M. Faust, K. Schaber, Influence of anion and cation on the vapor pressure of binary mixtures of water+ionic liquid and on the thermal stability of the ionic liquid, Fluid Phase Equilib. 394 (2015) 29–37, https://doi.org/10.1016/j.fluid.2015.03.001.
[21] L.E. Ficke, H. Rodríguez, J.F. Brennecke, Heat Capacities and Excess Enthalpies of 1-Ethyl-3-methylimidazolium-Based Ionic Liquids and Water, J. Chem. Eng. Data 53 (9) (2008) 2112–2119, https://doi.org/10.1021/je800248w.
[22] A.L. Saroj, R.K. Singh, Thermal, dielectric and conductivity studies on PVA/Ionic liquid [EMIM][$EtSO_4$] based polymer electrolytes, J. Phys. Chem. Solids 73 (2) (2012) 162–168, https://doi.org/10.1016/j.jpcs.2011.11.012.
[23] Y. Cao, Y. Chen, X. Sun, Z. Zhang, T. Mu, Water sorption in ionic liquids: kinetics, mechanisms and hydrophilicity, Phys. Chem. Chem. Phys. 14 (2012) 12252–12262, https://doi.org/10.1039/c2cp41798g.
[24] A. Broderick, Y. Khalifa, M.B. Shiflett, J.T. Newberg, Water at the Ionic Liquid-Gas Interface Examined by Ambient Pressure X-ray Photoelectron Spectroscopy, J. Phys. Chem. C 121 (13) (2017) 7337–7343, https://doi.org/10.1021/acs.jpcc.7b00775.
[25] L. Cammarata, S.G. Kazarian, P.A. Salter, T. Welton, Molecular states of water in room temperature ionic liquids, Phys. Chem. Chem. Phys. 3 (2001) 5192–5200, https://doi.org/10.1039/b106900d.
[26] D. Ghoshdastidar, S. Senapati, Nanostructural Reorganization Manifests in Sui-Generis Density Trend of Imidazolium Acetate/Water Binary Mixtures, J. Phys. Chem. B 119 (34) (2015) 10911–10920, https://doi.org/10.1021/acs.jpcb.5b00433.
[27] K. Dong, S. Zhang, J. Wang, Understanding the hydrogen bonds in ionic liquids and their roles in properties and reactions, Chem. Commun. 52 (41) (2016) 6744–6764, https://doi.org/10.1039/C5CC10120D.
[28] L.A.S. Ries, F.A. do Amaral, K. Matos, E.M.A. Martini, M.O. de Souza, R.F. de Souza, Evidence of change in the molecular organization of 1-n-butyl-3-methylimidazolium tetrafluoroborate ionic liquid solutions with the addition of water, Polyhedron 27 (15) (2008) 3287–3293, https://doi.org/10.1016/j.poly.2008.07.029.
[29] D.A. Turton, J. Hunger, A. Stoppa, G. Hefter, A. Thoman, M. Walther, R. Buchner, K. Wynne, Dynamics of imidazolium ionic liquids from a combined dielectric relaxation and optical Kerr effect study: evidence for mesoscopic aggregation, J. Am. Chem. Soc. 131 (31) (2009) 11140–11146, https://doi.org/10.1021/ja903315v.
[30] P.M. Lalli, Y.E. Corilo, G.F. de Sa, R.J. Daroda, V. de Souza, G.H.M.F. Souza, I. Campuzano, G. Ebeling, J. Dupont, M.N. Eberlin, Intrinsic mobility of gaseous cationic and anionic aggregates of ionic liquids, ChemPhysChem 12 (8) (2011) 1444–1447, https://doi.org/10.1002/cphc.201100099.

[31] K.N. Ruckart, R.A. O'Brien, S.M. Woodard, K.N. West, T.G. Glover, Porous Solids Impregnated with Task-Specific Ionic Liquids as Composite Sorbents, J. Phys. Chem. C 119 (35) (2015) 20681–20697, https://doi.org/10.1021/acs.jpcc.5b04646.
[32] K. Fatyeyeva, S. Rogalsky, O. Tarasyuk, C. Chappey, S. Marais, Vapour sorption and permeation behaviour of supported ionic liquid membranes, React. Funct. Polym. 130 (2018) 16–28, https://doi.org/10.1016/j.reactfunctpolym.2018.05.007.
[33] R. Sood, C. Iojoiu, E. Espuche, F. Gouanvé, G. Gebel, H. Mendil-Jakani, S. Lyonnard, J. Jestin, Proton Conducting Ionic Liquid Doped Nafion Membranes, J. Phys. Chem. C 116 (2012) 24413–24423, https://doi.org/10.1021/jp306626y.
[34] F. Radakovitsch, F. Heym, A. Jess, Gas Drying Using Supported Ionic Liquids, Chem. Eng. Trans. 69 (2018) 667–672, https://doi.org/10.3303/CET1869112.
[35] F.R. Radakovitsch, A. Jess, Gas dehydration using the ionic liquid [EMIM][$MeSO_3$] supported on silica gel – Structural and water vapor sorption properties, Chem. Eng. J. 398 (2020) 124689, https://doi.org/10.1016/j.cej.2020.124689.
[36] E. Alcalde, I. Dinarès, A. Ibáñez, N. Mesquida, A simple halide-to-anion exchange method for heteroaromatic salts and ionic liquids, Molecules 17 (2012) 4007–4027, https://doi.org/10.3390/molecules17044007.
[37] I. Chiarotto, L. Mattiello, F. Pandolfi, D. Rocco, M. Feroci, NHC in Imidazolium Acetate Ionic Liquids: Actual or Potential Presence?, Front Chem. 6 (2018) 355, https://doi.org/10.3389/fchem.2018.00355.
[38] M.T. Clough, K. Geyer, P.A. Hunt, J. Mertes, T. Welton, Thermal decomposition of carboxylate ionic liquids: trends and mechanisms, Phys. Chem. Chem. Phys. 15 (2013) 20480–20495, https://doi.org/10.1039/c3cp53648c.
[39] J. Slattery, C. Daguenet, P. Dyson, T.S. Schubert, I. Krossing, How to predict the physical properties of ionic liquids: a volume-based approach, Angew. Chem. Int. Ed. 46 (28) (2007) 5384–5388, https://doi.org/10.1002/anie.200700941.
[40] M.A. Rocha, M.B. Shiflett, Water Sorption and Diffusivity in [C_2C_1im][BF_4], [C_4C_1im][OAc], and [C_4C_1im][Cl], Ind. Eng. Chem. Res. 58 (4) (2019) 1743–1753, https://doi.org/10.1021/acs.iecr.8b05689.
[41] Y. Chen, Y. Cao, Y. Zhang, T. Mu, Hydrogen bonding between acetate-based ionic liquids and water: Three types of IR absorption peaks and NMR chemical shifts change upon dilution, J. Mol. Struct. 1058 (2014) 244–251, https://doi.org/10.1016/j.molstruc.2013.11.010.
[42] Q. Berrod, F. Ferdeghini, J.-M. Zanotti, P. Judeinstein, D. Lairez, V. García Sakai, O. Czakkel, P. Fouquet, D. Constantin, Ionic Liquids: evidence of the viscosity scale-dependence, Sci. Rep. 7 (2017) 2241, https://doi.org/10.1038/s41598-017-02396-7.
[43] T. Burankova, R. Hempelmann, A. Wildes, J.P. Embs, Collective ion diffusion and localized single particle dynamics in pyridinium-based ionic liquids, J. Phys. Chem. B 118 (49) (2014) 14452–14460, https://doi.org/10.1021/jp5092416.
[44] A. Wexler, S. Hasegawa, Relative Humidity-Temperature Relationships of Some Saturated Salt Solutions in the Temperature Range 0° to 50° C, J. Res. Natl. Bur. Stand. 53 (1954) 19–26, https://doi.org/10.6028/jres.053.003.
[45] W. Xie, X. Ji, X. Feng, X. Lu, Mass Transfer Rate Enhancement for CO_2 Separation by Ionic Liquids: Effect of Film Thickness, Ind. Eng. Chem. Res. 55 (1) (2016) 366–372, https://doi.org/10.1021/acs.iecr.5b03339.
[46] M. Mirzaei, A.R. Badiei, B. Mokhtarani, A. Sharifi, Experimental study on CO2 sorption capacity of the neat and porous silica supported ionic liquids and the effect of water content of flue gas, J. Mol. Liq. 232 (2017) 462–470, https://doi.org/10.1016/j.molliq.2017.02.104.
[47] J. Lemus, J. Palomar, M.A. Gilarranz, J.J. Rodriguez, Characterization of Supported Ionic Liquid Phase (SILP) materials prepared from different supports, Adsorption 17 (3) (2011) 561–571, https://doi.org/10.1007/s10450-011-9327-5.